

Possibilities and Limitations of the Tomographic Method for verification of the Integrity of Spent Nuclear Fuel

by Camilla Andersson

Abstract:

A tomographic method, using algebraic reconstruction methods, has been examined for verification of the integrity of spent nuclear fuel. Computer simulations were performed where fuel rods have been removed, i.e. water filled, or replaced with fuel-like material. Various geometric patterns of removed or replaced rods have been examined both for BWR and PWR fuel. Two gamma energies, 662 keV from ^{137}Cs and 1274 keV from ^{154}Eu , have been used in the simulations. It is shown that the higher energy was favourable due to its higher penetrability. Various measurement strategies have been examined especially concerning the number of measurements and the level of statistical noise. The simulations point at the possibility of detecting tampering of a fuel assembly on a single rod level. The replacement with fresh fuel or fuel-like material lead to more confident detection of the manipulation comparing to the case where rods have been replaced with water.

TABLE OF CONTENTS

ABSTRACT:	1
CHAPTER 1. INTRODUCTION	3
CHAPTER 2 METHOD	3
2.1 SINGLE PHOTON EMISSION COMPUTED TOMOGRAPHY (SPECT)	3
2.2 ALGEBRAIC RECONSTRUCTION ALGORITHMS	4
2.3 EFFECTS DUE TO STRONG ATTENUATION	5
CHAPTER 3 SIMULATIONS	7
3.1 GEOMETRY USED IN THE SIMULATIONS	7
3.2 STATISTICAL NOISE	7
CHAPTER 4 RECONSTRUCTIONS	8
4.1 NUMBER OF ITERATIONS	8
4.2 THE RELAXATION PARAMETER	8
4.3 QUALITY PARAMETERS	8
CHAPTER 5 RESULTS	10
5.1 RODS REMOVED OR REPLACED IN BWR FUEL	10
5.1.1 <i>Single rods</i>	11
5.1.2 <i>The inner section</i>	17
5.1.3 <i>The chess pattern</i>	22
5.1.4 <i>Comparison between the ¹⁵⁴Eu and ¹³⁷Cs gamma energies</i>	25
5.2 RODS REMOVED OR REPLACED IN PWR FUEL	26
5.2.1 <i>Single rods</i>	27
5.2.2 <i>Groups of rods</i>	30
5.3 COMPARISONS BETWEEN PWR AND BWR	33
CONCLUSIONS	34
REFERENCES:	34
ACKNOWLEDGMENTS:	34

Chapter 1. Introduction

The intended final storage of nuclear fuel in Sweden requires a method for verifying the integrity¹ of spent nuclear fuel. The development of a tomographic method for verifying the integrity has been reported in ref. 2. In this report investigations using that method have been made by performing computer simulations. The possibilities of replacing rods with fresh fuel or fuel-like material; or removing rods without replacing them, hence water filled positions, have been treated. Two different types of fuel have been investigated, BWR (*Boiling Water Reactor*) and PWR (*Pressure Water Reactor*).

In the fission process, the fission products ^{154}Eu and ^{137}Cs are produced. These radioactive isotopes beta-decay and emit gamma-quanta with typical energies of 1274 keV and 662 keV, respectively. These two isotopes are interesting since they appear in large concentrations and have comparably long half-lives, 8.5 years for ^{154}Eu and 30 years for ^{137}Cs . The tomographic method used here is called *Single Photon Emission Computed Tomography* (SPECT) where the gamma intensities are detected in a large number of positions and subsequently used for reconstructing the activity distribution. An algebraic reconstruction algorithm called ART, *Algebraic Reconstruction Technique*, is used to calculate the activity in each rod.

In ref. 2, the possibility of detecting the water channel in a BWR fuel assembly, with no prior knowledge of its position, has been thoroughly investigated including the influence from various parameters. The detection of both replaced and removed rods in various patterns have been investigated; three main patterns for BWR and two for PWR. The replacement with fresh fuel implies the same attenuation of the gamma radiation as in an intact fuel element, while the presence of water implies a different attenuation than the one presumed. It was shown that the change in attenuation leads to somewhat less accurate in the result due to the dependence of the tomographic method on the presumed attenuation.

Chapter 2 Method

This chapter describes some of the most fundamental aspects and concepts of the tomographic method and the reconstruction technique studied in this work. More detailed information is given in references 2, 3 and 4.

2.1 Single photon emission computed tomography (SPECT)

In SPECT the emitted gamma radiation from a radioactive isotope in a section of an object is used for imaging the spatial distribution of the isotope. The number of gamma quanta emitted per second per unit volume is proportional to the concentration of the source in that volume. The collimator-detector system defines which parts of the object that will contribute to the intensity in a certain measurement, see figure 1. By performing measurements in various positions relative the object, projection data are collected that are used in the reconstructions algorithms.

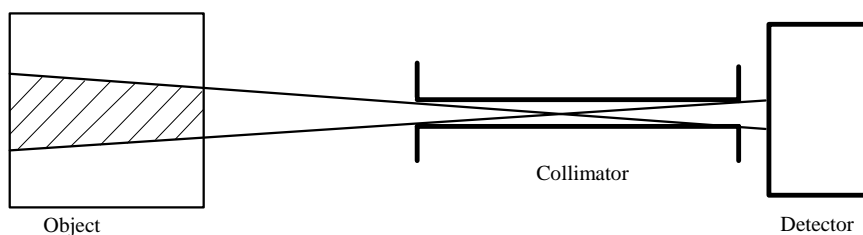


Figure 1. A collimator system defining the parts of an object contributing to the intensity in the detector.

¹ The word integrity is used to account for the fact that assemblies may be reconstructed in such way that the original rods have been replaced or removed. /ref. 1/. Such action may take place both legally and illegally, e.g. in order to steal nuclear material.

SPECT is complicated if the attenuation of the photons varies along their way from the source to the detector. In the case of large attenuation, algebraic reconstruction methods are therefore preferred, since in that case they are reported to give more accurate results than present analytic reconstruction methods, such as the Radon transform /ref. 3/.

2.2 Algebraic reconstruction algorithms

The algebraic reconstruction algorithms are useful when the radiation may be subject to strong attenuation between the source and the detector. The object is divided into smaller parts, so called *picture elements* or *pixels* and the activity in each pixel is reconstructed. So called *contribution coefficients*, w_{mn} , can be introduced which describe that out of the total activity A_n in pixel n , only $A_n \cdot w_{mn}$ photons will reach the detector in position m each second. The contribution coefficients depend on attenuation and geometric factors. The M measurements give rise to an equation system where the number of unknown quantities, A_n , equals the number of pixels, N .

$$\begin{pmatrix} w_{11} & w_{12} & w_{13} & \cdots & w_{1N} \\ w_{21} & w_{22} & w_{23} & \cdots & w_{2N} \\ w_{31} & w_{32} & w_{33} & \cdots & w_{3N} \\ \vdots & & & & \\ w_{M1} & w_{M2} & w_{M3} & \cdots & w_{MN} \end{pmatrix} \cdot \begin{pmatrix} A_1 \\ A_2 \\ A_3 \\ \vdots \\ A_N \end{pmatrix} = \begin{pmatrix} I_1 \\ I_2 \\ I_3 \\ \vdots \\ I_M \end{pmatrix} \quad (\text{eq. 1})$$

The equation system is solved by setting a start activity to each pixel, A_n , and then performing iterative corrections of all activities to match the measured intensities, I_m . Different algebraic algorithms use different ways of making the corrections. In this work the so called ART method (Algebraic Reconstruction Technique) /ref. 4/ has been used. During an iteration the activity values are corrected according to:

$$A_n^{\text{new}} = A_n^{\text{old}} - \frac{w_{mn}}{\sum_n w_{mn}^2} \cdot \Delta I_m \quad (\text{eq. 2})$$

where:

$$\Delta I_m = I_m^{\text{calculated}} - I_m^{\text{measured}} \quad (\text{eq. 3})$$

This procedure is however sensitive to statistical noise that might cause large fluctuations of the reconstructed values. It is therefore relevant to introduce a relaxation parameter R_p with a value between 0 and 1 to stabilise the iteration process. Equation 2 is changed to

$$A_n^{\text{new}} = \begin{cases} A_n^{\text{old}} - R_p \frac{w_{mn}}{\sum_n w_{mn}^2} \Delta I_m \\ 0, \text{ if the expression above is less than } 0 \end{cases} \quad \text{or} \quad (\text{eq. 2'})$$

An iteration is complete when all the activities have been corrected for all measurements. Many iterations may be needed until a sufficiently accurate solution is obtained.

2.3 Effects due to strong attenuation

The geometry of the nuclear fuel assembly is known in detail and the absorption matrix can be calculated from the geometrical dimensions and attenuation constants for each material. The average value of the attenuation is high which may lead to problems of detecting inner rods since they only contribute with a small part of the total detected intensity.

The attenuation constant μ for different materials and energies

Energy	Fuel (m ⁻¹)	Zircalloy-2 (m ⁻¹)	Zircalloy-4 (m ⁻¹)	Water (m ⁻¹)
¹³⁷ Cs (662 keV)	121.734	46.509	46.513	8.538
¹⁵⁴ Eu (1274 keV)	62.72	32.932	32.931	6.239

Table 1. The values above are calculated from the given values received from ref. 5,6 and 7. Zircalloy-2 is used in BWR fuel and Zircalloy-4 is used in PWR-fuel.

If a rod is removed, the presumed absorption matrix will be incorrect. This change will lead to an error in the reconstructed activity. The fact that the position contains water instead of fuel will also lead to higher contributions to the measured intensities from the adjacent rods. These facts imply that the reconstructed activity in the position of a removed rod will be substantial. If the position instead contains fresh fuel the assumed attenuation is correct and the reconstructed activity in such a position can be expected to be close or equal to zero.

The average attenuation coefficients of a fuel assembly at two different gamma energies are shown in table 2.

Average attenuation coefficient	Cs -137 (m ⁻¹)	Eu -154 (m ⁻¹)
μ_{BWR}	51.130	28.467
μ_{PWR}	48.226	26.789

Table2. The average attenuation coefficients are calculated using the attenuation values from table 1. times the corresponding fraction of the whole volume content.

Using the values given in table 2 it is possible to calculate a rough estimate of the intensity fraction of each rod using equation 4.

$$I = I_0 e^{-\mu d} \quad (\text{eq. 4})$$

where *I* is the measured intensity
*I*₀ is the original intensity
 μ is the attenuation constant
d is the distance through which the attenuation takes place

The formula can also be described as a function of rows:

$$I = I_0 e^{-\mu(a/2+na)} \quad (\text{eq. 4'})$$

where a is the distance between two rods
 n is the number of rows that the radiation passes

The results of these calculation are presented in tables 3a) and b). The figures correspond to the fraction of the gamma quanta from a rod emitted perpendicularly to the assembly side that escapes the assembly.

BWR fuel		
The escape fraction in percent.		
row	Cs-137	Eu-154
1	66.4	79.6
2	29.3	50.5
3	12.9	32.0
4	5.7	20.3
5	2.5	12.9
6	1.1	8.2
7	0.5	5.2
8	0.2	3.2

Table 3a) The escape fraction of gamma quanta from different rows emitted approximately perpendicular to the assembly side.

PWR fuel		
The escape fraction in percent.		
row	Cs-137	Eu-154
1	73.8	84.5
2	40.2	60.3
3	21.9	43.0
4	11.9	30.7
5	6.7	22.2
6	3.5	15.6
7	1.9	11.1
8	1.0	8.0
9	0.6	5.7
10	0.3	4.0
11	0.2	2.9
12	0.1	2.1
13	0.1	1.5
14	0.0	1.0
15	0.0	0.8
16	0.0	0.5
17	0.0	0.4

Table 3b) The escape fraction of gamma quanta from different rows emitted approximately perpendicular to the assembly side.

As shown in tables 3a) and b), the large attenuation results in very small contributions from the inner rods, especially for PWR fuel. Consequently it can be expected that the inner rods are the most difficult to reconstruct.

Chapter 3 Simulations

The investigations in this report are based upon simulated data since actual measurements would be very time consuming and expensive at this stage. The equation system in section 2.2 (eq. 1) has been used for such simulations by setting an activity to each pixel and performing the matrix multiplication. Before using the intensities in the reconstructions statistical noise has been added.

3.1 Geometry used in the simulations

The geometry used in the simulation is shown in figure 2 and table 4.

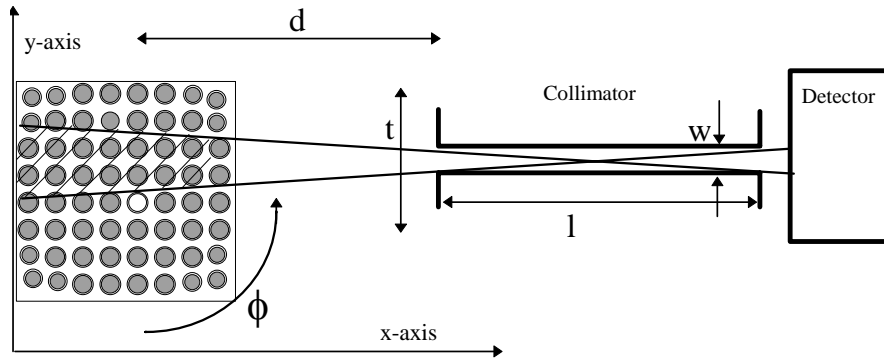


Figure 2. The simulated equipment, here containing a BWR fuel assembly. The angle ϕ , corresponds to the rotational position, t corresponds to the transverse position of the collimator along the y -axis; d is the distance from the centre of the assembly to the front of the collimator, l is the length of the collimator and w the width of the collimator.

Quantity	BWR	PWR
d	15 cm	24 cm
l	30 cm	30 cm
w	2 mm	2 mm

Table 4. Values used in the simulations. See fig. 2. Φ and t were varied in each simulation in order to simulate measurements in various positions.

The start value of Φ and the number of angular positions as well as the number of translations have been varied to study their effect on the result. The total number of angular positions and translations is called the number of positions.

3.2 Statistical noise

To conform with an experimental situation statistical noise has been added to the calculated intensities. In the experimental situation, the measuring time in each position (Φ , t) is considered equal. The added noise is based upon the one position that gives the highest intensity which is then set as the value of the parameter N_{\max} , i.e. the highest number of collected counts in any measurement. The square root of N_{\max} is the standard deviation of the of statistical fluctuations in that a measurement.

Chapter 4 Reconstructions

To reconstruct the activity distribution the generated intensities, including statistical noise, were used as input together with the absorption matrix as described in section 2.2. To calculate the activity values the program was supplied with a tentatively set activity distribution and the matrix multiplication of eq 2.2 was performed. A comparison between the generated intensities and the calculated intensities was made after which the activity distribution was corrected using eq.2'. This procedure was repeated until a stable result was achieved. No information about replaced or removed rods was assumed to be available and the ability to discern such rods was studied.

4.1 Number of iterations

The reconstructions were performed by iterating a pre-selected number of times. The activities were displayed for inspections with certain intervals making a stabilisation control possible. In the investigations presented here every third iteration out of totally 100 and every 10:th iteration out of totally 500 for BWR and PWR respectively, have been displayed for controlling the stability. The changes between consecutive iterations were then smaller than 1‰.

4.2 The relaxation parameter

A relaxation parameter, $0 < R_p < 1$, was introduced in order to make the iteration process more robust, see eq. 2'. In this case $R_p=0.05$ has been chosen for the PWR case and the expression below for BWR:

$$R_p = \frac{1}{\left\langle \frac{\text{iterationnumber}}{10} \right\rangle}$$

Where $\langle \rangle$ means the expression in the brackets should be rounded off to the smallest integer greater than or equal to its argument, e.g. $\langle 3.2 \rangle$ becomes 4.

In the case of PWR, which was not investigated in ref. 2, a constant value was chosen since no information was known about the convergence of the iteration process. The above definition of R_p in the case of BWR has the advantage that the changes in the beginning are larger and become progressively smaller with increasing number of iterations. As a consequence the quality of the reconstruction will improve. The speed of the convergence is however likely to slow down somewhat, due to the fact that large changes of the activities are prohibited. A false stabilisation could therefore be visible in some cases/ref. 4/.

4.3 Quality parameters

As a measure of agreement between the reconstructed and simulated activity of each fuel rod, two parameters have been used.

- i) The relative standard deviation, s , of the reconstructed values of the activities.
- ii) The relative deviation of the reconstructed activity of a removed or replaced fuel rod from the mean activity of all other fuel rods, Δ .

Δ is defined as:

$$\Delta = \frac{A}{\hat{A}}$$

where: A = The activity of a rod presumed to be replaced or removed in the simulation.

$$\hat{A} = \frac{\sum A_i}{\sum i}, \quad A_i = \text{The reconstructed activity of a fuel rod not belonging to the above category.}$$

The standard deviation s is defined as :

$$s = \frac{\sigma}{\hat{A}}$$

where: σ is the standard deviation calculated for all rods that are presumed not replaced or removed.
 \hat{A} as defined above

A minimisation of both Δ and s is desired.

In cases where more than one rod is replaced only the largest value of the parameter Δ , Δ_{\max} and the mean value, Δ_{mean} have been accounted for in section 5.

Chapter 5 Results

In this section the results of simulations of various configurations of replaced rods in BWR and PWR fuel assemblies are presented. For the BWR fuel three cases are presented and for the PWR fuel two cases. The two parameters, s and Δ defined in section 4.3, are used as a measure of the quality of the results.

5.1 Rods removed or replaced in BWR fuel

The BWR fuel assemblies have a square shape with the side 0.138 m and contain 63 fuel rods and one water channel, see figure below. Since the area of the corner rods for BWR are approximately 10 % smaller, the reconstructed activities has been adjusted correspondingly when calculating the quality parameters. In the investigations it is desirable to examine as much as possible of the assembly, so the translations start at one corner of the fuel and move in small steps over to the opposite corner. The fuel is then rotated and the process is repeated. In section 3.1 information about the geometry of the simulated equipment is given.

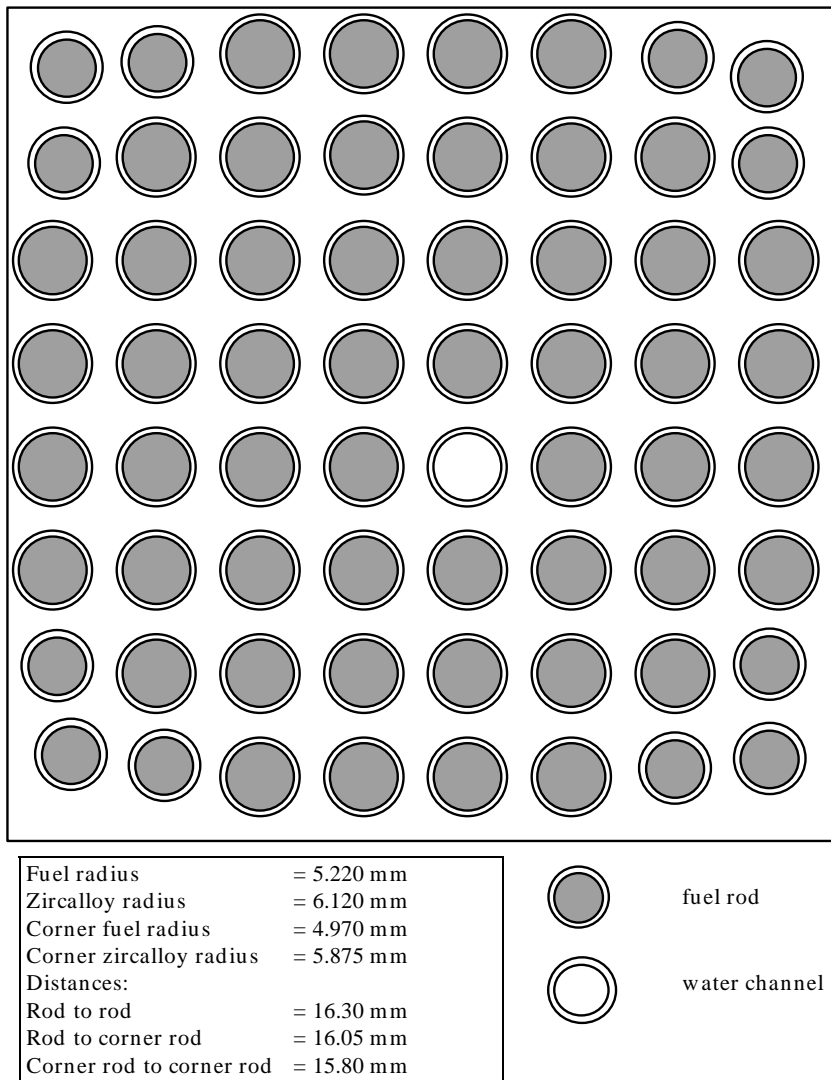


Figure 3. Schematic picture of a BWR fuel assembly. This assembly is complete and contains 63 fuel rods and one water channel. It has a square shape with the side 13.8 cm. The corner rods are smaller than the ordinary fuel rods. Because of the constant specific activity assumed, the reconstructed activity in these corner rods will be smaller than in all other rods.

The simulated measurements have been made mostly using a gamma energy of 662 keV, corresponding to the decay of ^{137}Cs and to a small extent using 1274 keV, corresponding to the decay of ^{154}Eu .

A few thorough investigations have been made to establish the relation between the standard deviation, s , and the number of measurement positions. Also the relation between s and N_{max} have been investigated. Investigations have also been made to how of the value of Δ , the reconstructed activity in the removed or replaced rods, varies. Three geometric formations of removed or replaced rods have been studied; single rods in various positions, the central section (4x4 rods) and a chess-like pattern in the middle of the assembly.

5.1.1 Single rods

Disregarding the water channel, the rods in BWR fuel form a symmetric 8x8 matrix. Using this symmetry the fuel can be divided by four symmetry lines into eight parts, each containing six whole rods and four that are shared diagonally with a neighbour, see fig. 4. These ten positions have been examined and the results are presented below.

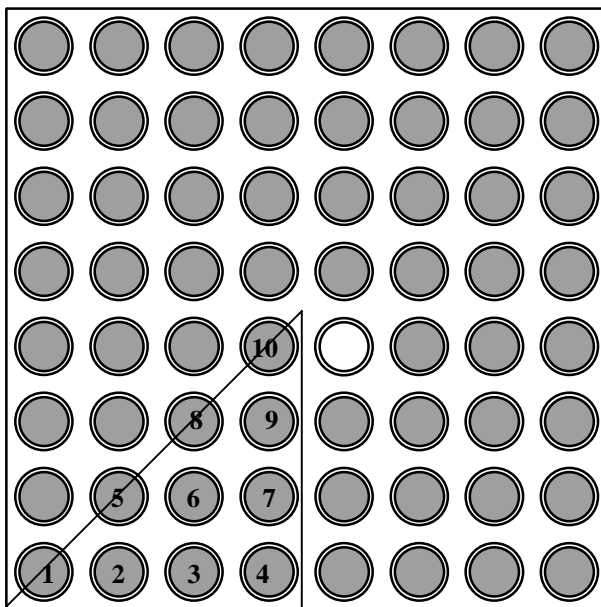


Figure 4. The eight-fold symmetry triangles of which the marked triangle is examined. The numbers of the rods correspond to the position on the x-axis in fig 7.

It is essential to treat each eighth identically, otherwise the symmetry is not valid. Therefore the number of angles used was divisible by eight, so that each eighth was investigated using equally many measurement positions.

Investigation of the s with various number of detector positions and levels of statistical noise.

An investigation of how the standard deviation depends on the number of measurement positions and the maximum number of counts in any measurement N_{max} has been made for BWR fuel in which one corner rod has been removed or replaced. The standard deviation decreases as expected when the number of measurement positions increases. It is also evident that s decreases when N_{max} increases. This is shown in the diagrams below.

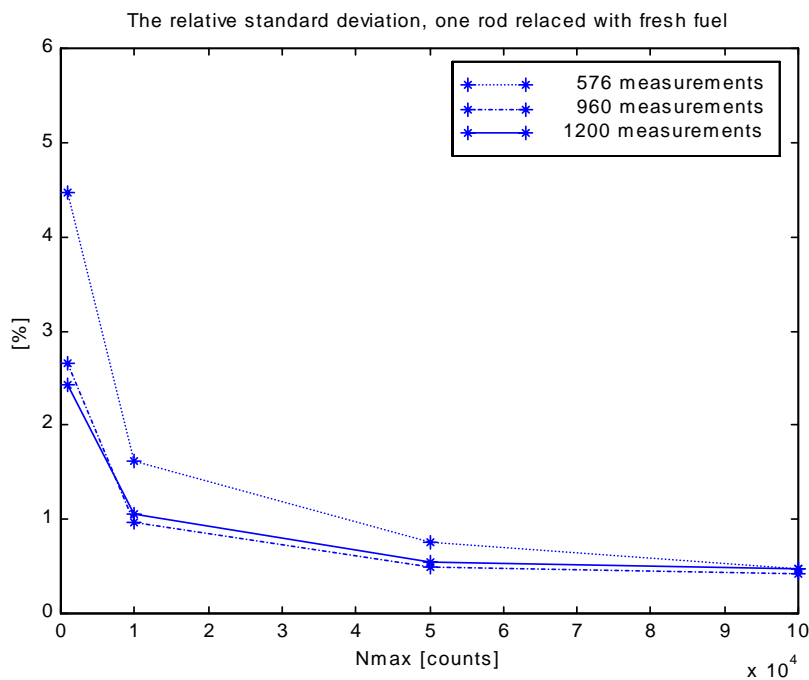
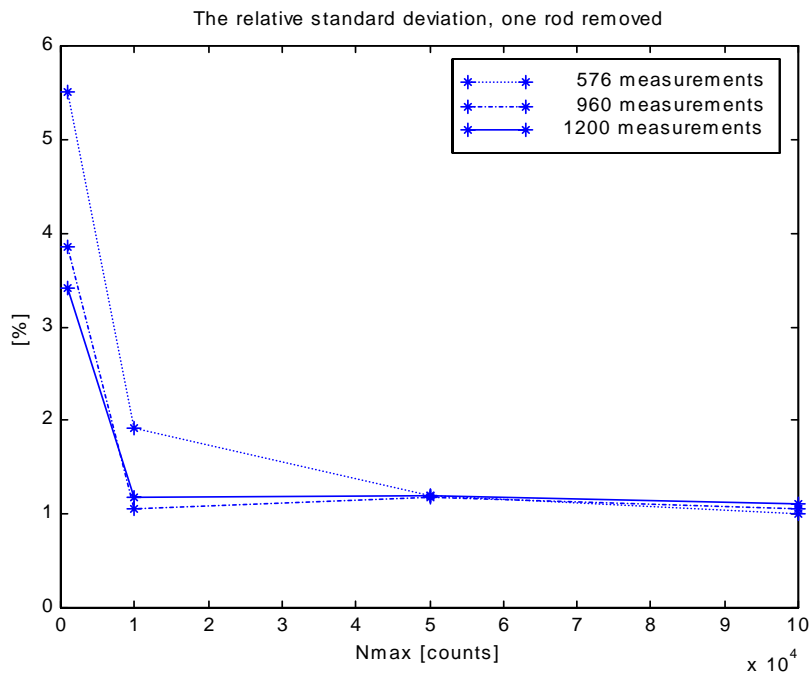


Figure 5a) and b). The standard deviation s as a function of the number of measured counts. The replaced rod is a corner rod. In a) the rod has been replaced with water and in b) the rod has been replaced with fresh fuel.

In figure 5 b) above it is obvious that the standard deviation is smaller when the presumed attenuation is correct, i.e. the case where rods are replaced with fresh fuel. It is also shown that an increasing number of collected counts, i.e. higher N_{\max} , gives progressively smaller standard deviation.

The relation between the number of measurement positions and the relative standard deviation is shown in figure 6 for $N_{\max}=10000$ counts. It shows the expected behaviour, i.e. s decreases as the number of measurement positions increases.

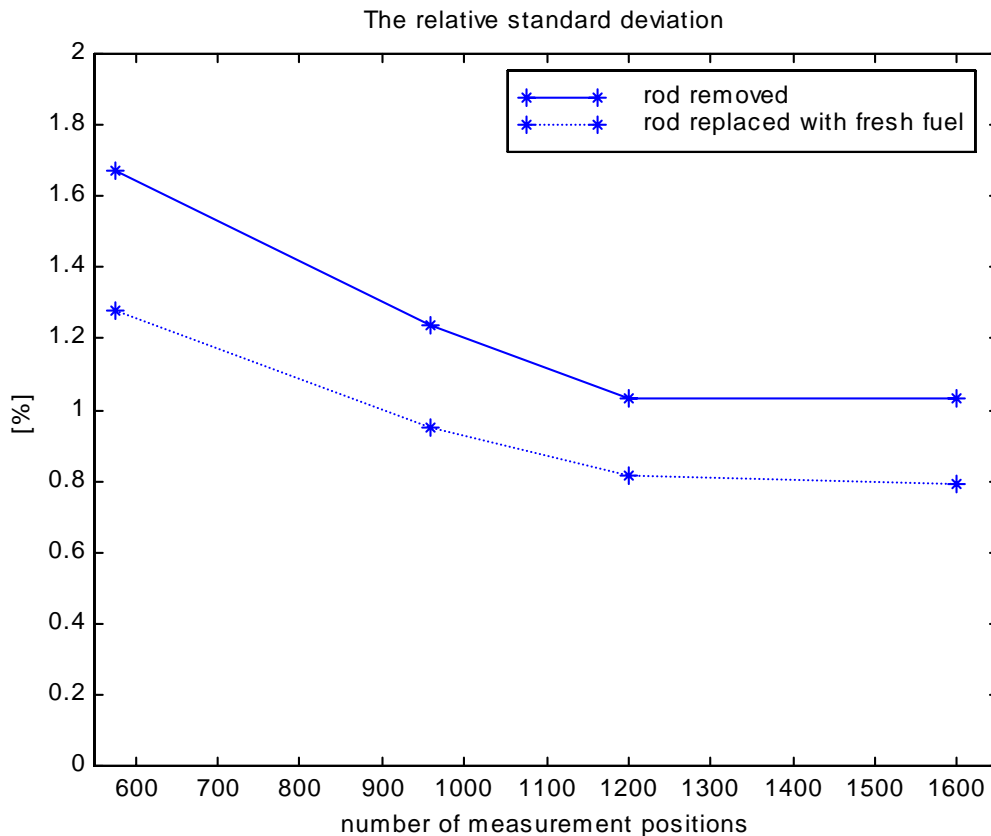


Figure 6. The standard deviation in percent as a function of the number of measurement positions. Both for the corner rod removed and replaced with fresh fuel.

In fig. 6 the importance of a correct attenuation is shown, as the standard deviation is smaller when assuming the attenuation correctly. Below is a figure describing the Δ values corresponding to the case of the standard deviation in fig. 5a), i.e. with one corner rod removed. There is no large variation in Δ in contrast to the appearance of the standard deviation in the same case.

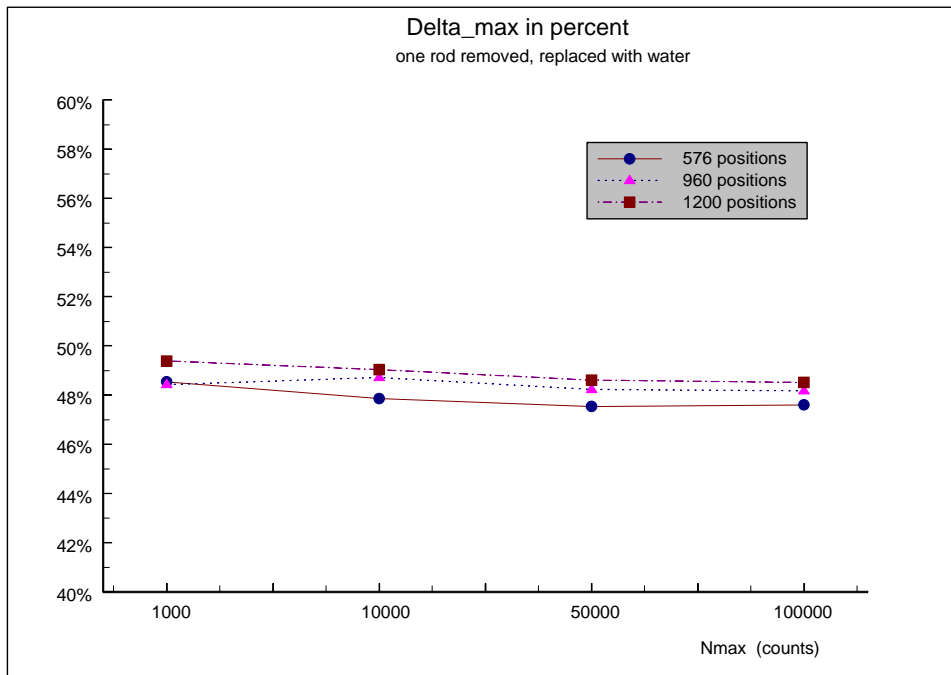


Figure 7. The Δ values for three sets of positions as a function of N_{max} . From the figure we conclude that changes in of Δ was at most about 2% regardless of the number of position or the value of N_{max} .

Comparisons between rods removed or replaced in ten different positions.

According to figures 5 and 6 1200 positions and $N_{max} = 10000$ counts, should give a standard deviation of about 1%, when measuring at 662 keV. These numbers have been used for investigating the possibilities of detecting removals or replacements of single rods in the remaining eight positions. The values of Δ and s for all these ten cases are found in figure 8a) and b) for removed rods and in figure 9a) and b) for rods replaced with fresh fuel.

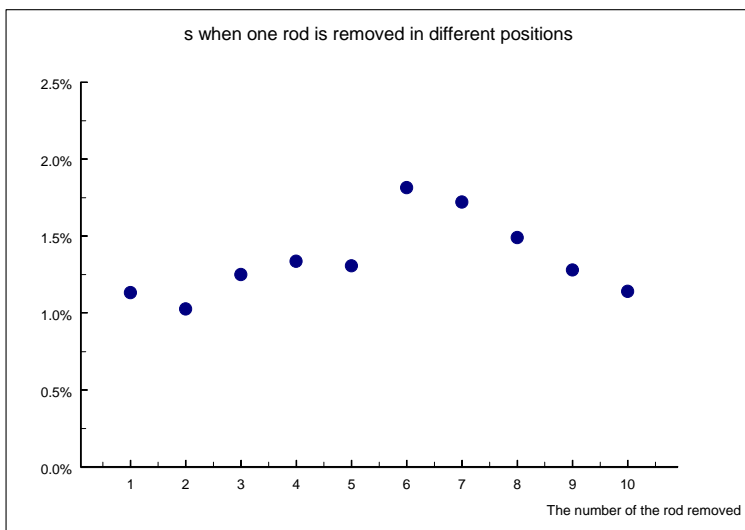
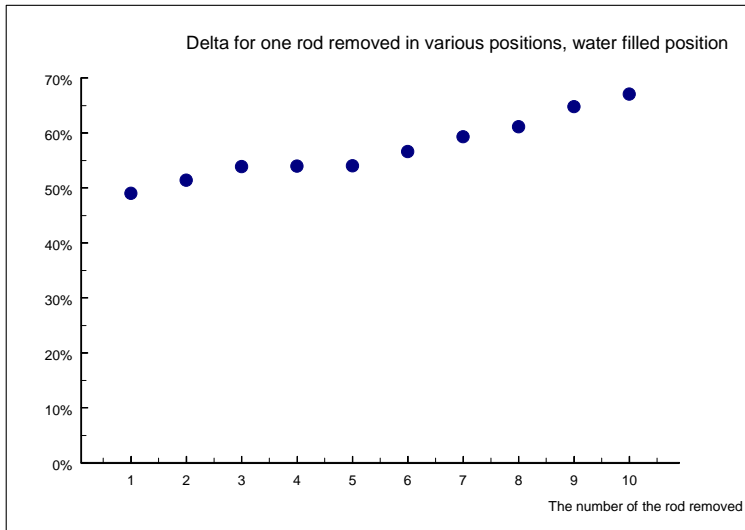


Figure 8 a) and b). In a) Δ for the removed rod is displayed in per cent. b) shows the corresponding standard deviations. All simulations are made at 662 keV using 1200 measurement positions and $N_{max} = 10000$ counts. The number on the x-axis refer to the rod number indicated in figure 4.

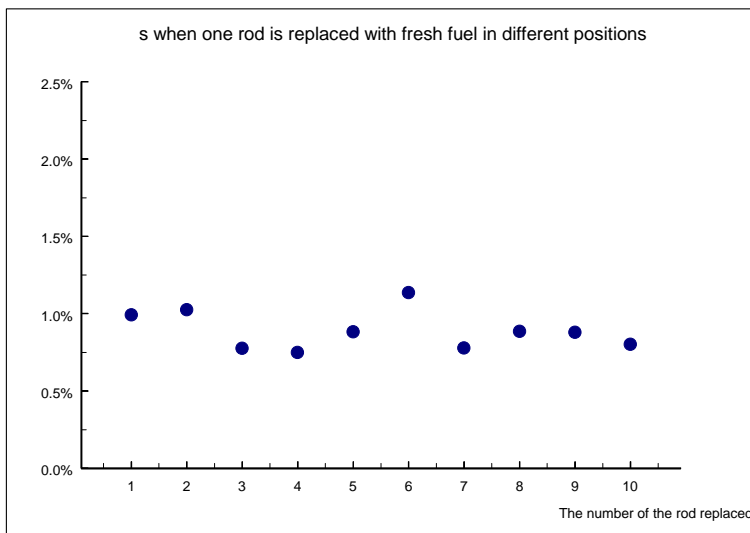
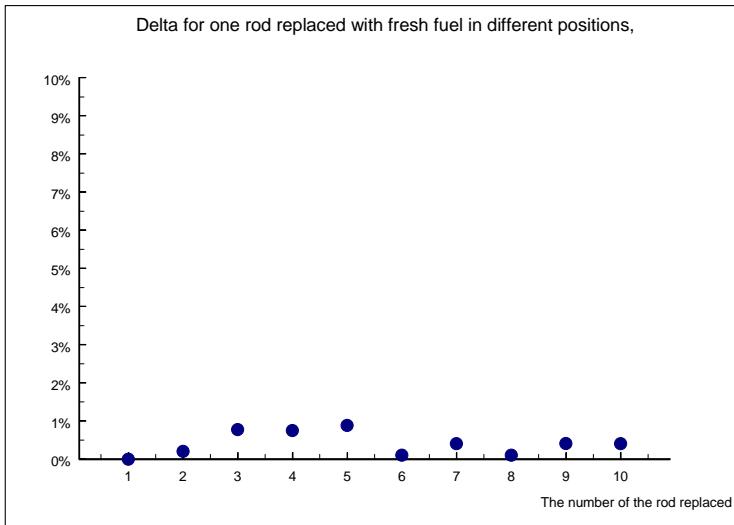


Figure 9 a) and b). In a) Δ for the replaced rods is displayed in per cent and b) show the corresponding standard deviations. All simulations are made at 662 keV using 1200 measurement positions and $N_{max} = 10000$ counts.

In fig 8a) it is obvious that Δ increases the more central the removed rod is, implying that it is easier to find a removed outer rod than an inner as expected in section 2.3. This difference is not apparent for rods replaced with fresh fuel in the BWR case. Here the Δ values are below 1% in all displayed cases. This is in line with the assumption in section 2.3 that this value should be equal or close to zero. The value of Δ for the water filled positions was in all cases below 70%, which is at least 15 standard deviations smaller than the mean value of the reconstructed activities. The standard deviation is in no single case larger than 2%.

5.1.2 The inner section.

The second main formation was rods removed or replaced in a group. Here the inner most 15 rods (not including the water channel) have been removed or replaced and several measurement strategies have been studied.

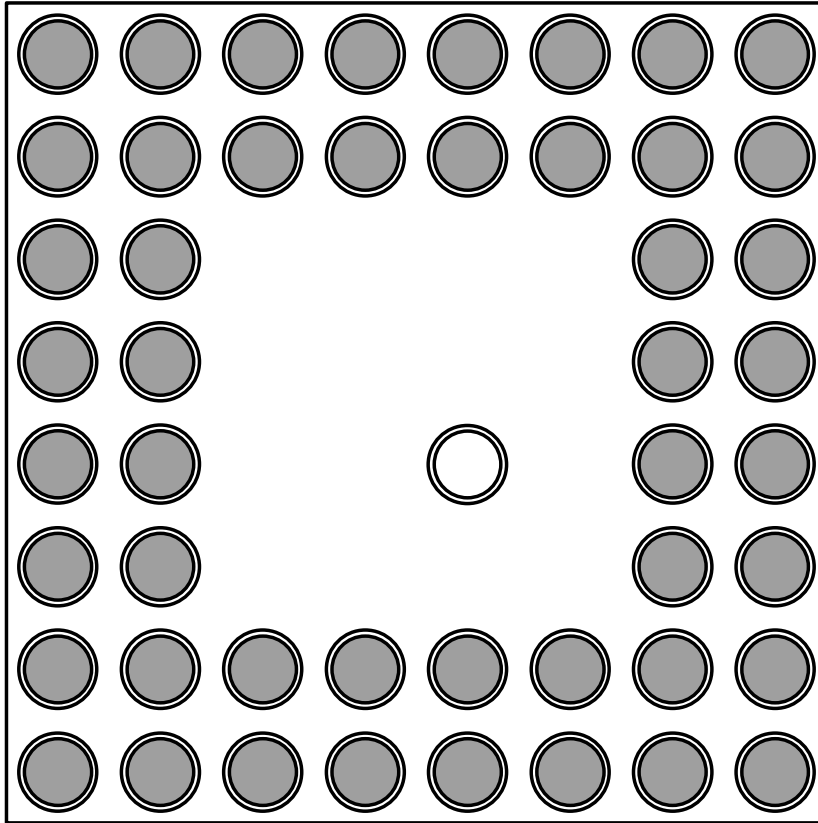


Figure 10 Schematic picture of the configuration in these investigations. The empty space represent the removed or replaced rods.

In most of the cases the gamma energy 662 keV (^{137}Cs) was used but one comparison with 1274 keV (^{154}Eu) was made. The results for ^{154}Eu is presented in chapter 5.2.4 where comparisons are made regarding nine BWR simulations made with both ^{154}Eu and ^{137}Cs .

The effect of an offset in the starting angle

In ref. 2 it was shown that an offset of 3° in the starting angle from a symmetry axis has a positive influence on the result in the case of one rod removed. A similar study has here been made for the case of removing the inner section. The results in fig. 11 show that the standard deviations s decreases significantly, i.e. with about 1.3 per cent units.

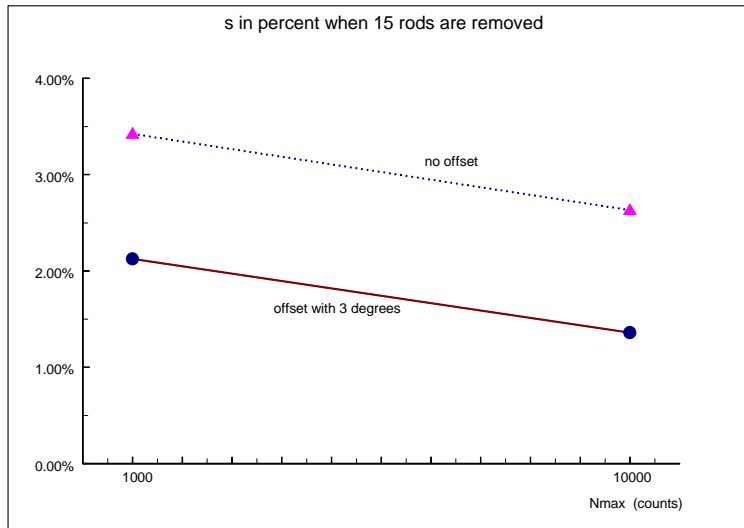


Figure 11. The effect of an offset in the starting angle is shown. The inner section has been removed according to fig. 10.

Figure 11 indicates the advantage of using an offset. It is evident that the offset of 3° produces a substantial decrease of the standard deviation. Also the Δ values show improve if an offset of 3° is used. Due to the positive effect of an offset, it has been used throughout the whole investigation.

Various numbers of detector positions and levels of statistical noise.

As is shown in figure 12 the parameter s is about 1% for 1200 positions and $N_{\max} = 10000$ counts, which is roughly the same as for one rod replaced. Similar results for 900 positions are shown in figure 13.

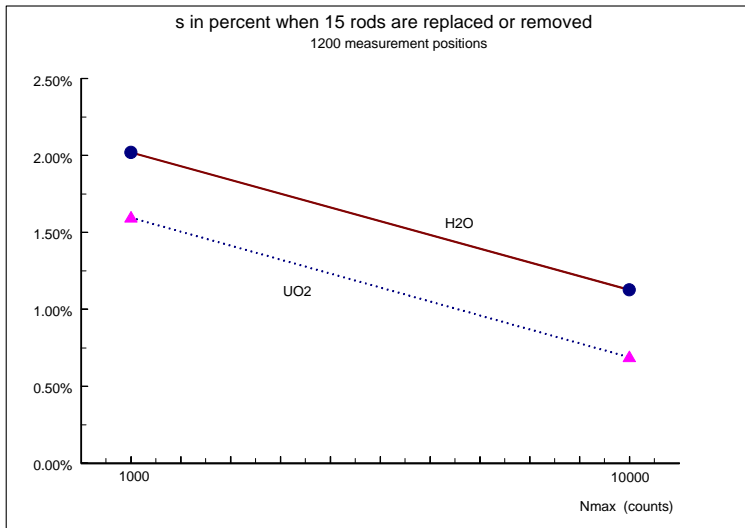


Fig. 12 The standard deviation for both the case of rods replaced with fresh fuel and the case with removed rods. Both cases have been calculated for 1200 positions and $N_{\max} = 10000$ counts.

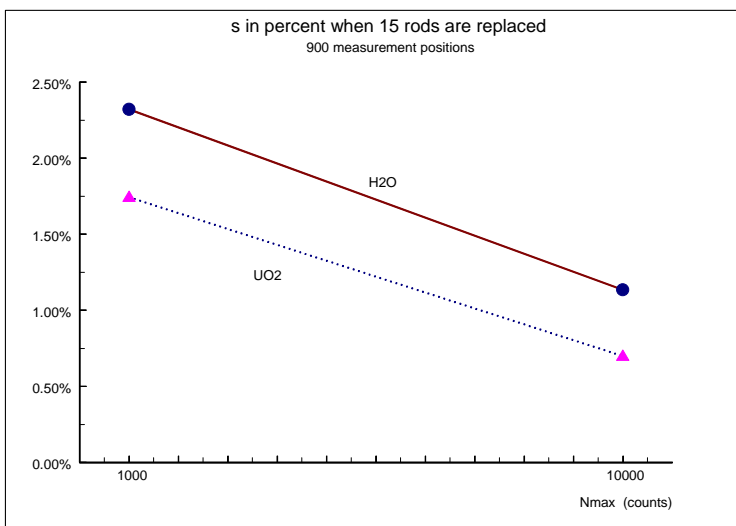


Figure 13. The parameter s as a function of N_{\max} . The same as in Fig 12 but the number of positions is fewer.

In Fig. 12 and 13 it is evident, just as in the case of one rod replaced, that the value of s is smaller when the rods have been replaced with fresh fuel compared to water filled positions. The diagrams also show that the parameter s is smaller as the number of measurement positions increases. When investigating Δ the result is comparable to the result for one rod replaced. The Δ value for rods replaced with fresh fuel is below 10%, which is reasonably close to the expected value of zero. In the case of removed rods Δ is higher, around 60%. The Δ values for removed rods, i.e. water filled positions are displayed below for different numbers of positions and N_{\max} .

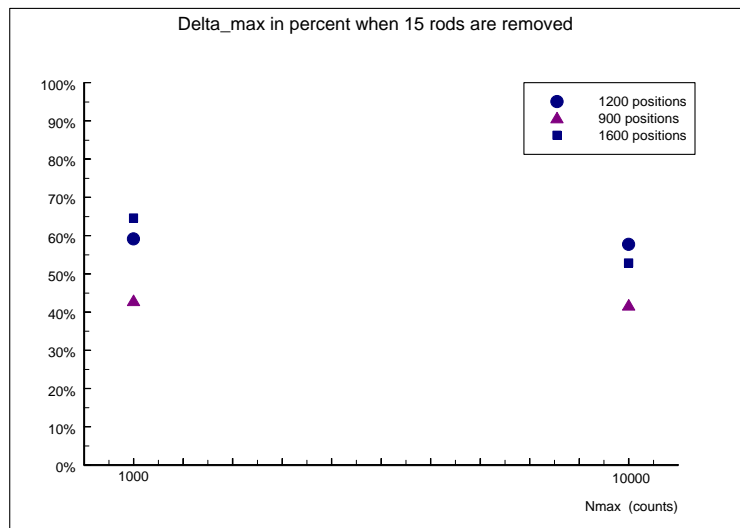


Figure 14. The maximum value of Δ , Δ_{\max} for 3 different numbers of positions.

In section 5.1.4 it is shown that the values of Δ for positions of rods replaced with water decrease with about 1/3 if ^{154}Eu radiation is used instead of ^{137}Cs .

Fig 14 shows that in the case of 900 detector positions (30 rotations x 30 translations) a much smaller value of Δ is obtained than for both 1200 and 1600 positions. This is not fully consistent with earlier results. The deviating results might be explained by detector positions with better views of the inner parts of the assembly.

Figure 15 shows the reconstructed activities for the case using 1600 positions and $N_{\max} = 10000$ counts.

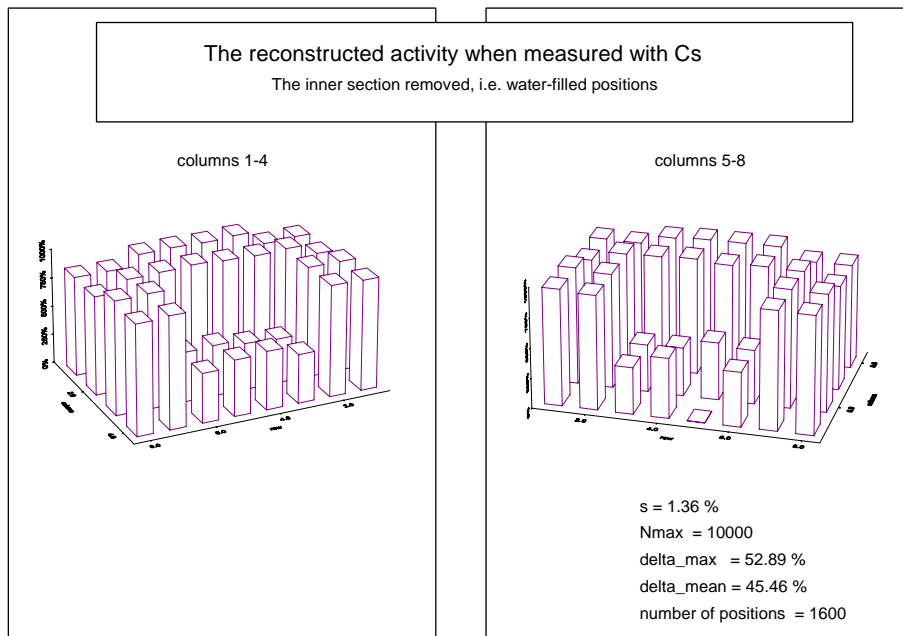


Figure 15. The actual reconstructed activities for each individual rod after 100 iterations when the inner section has been removed.

It is evident from figures 12, 13 and 14 that the large number of the replaced rods leads to smaller values of Δ than if single rods are replaced.

Also a study of removing the three inner most rods has been made, with results comparable to the results achieved in the study of the inner section (15 rods) removed using 1200 measurement positions and $N_{\max} = 10000$ counts were:

$$s = 1.1 \%$$

$$\Delta_{\text{mean}} = 66 \%$$

$$\Delta_{\text{max}} = 69 \%,$$

5.1.3 The chess pattern.

This configuration is similar to the one presented in 5.1.2. with the exception that the rods are now removed or replaced alternately, hence the name. Three configurations have been investigated for one set of positions and the two energies ^{137}Cs and ^{154}Eu .

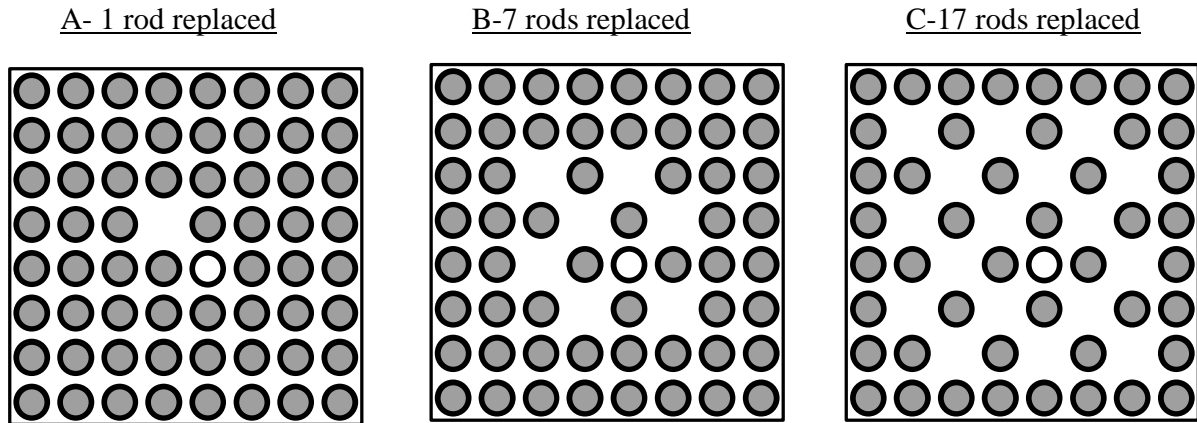


Figure 16 Three configurations of rods replaced in a the chess-pattern.

In fig. 17 the values of Δ and s for the removal of the three formations A,B and C are displayed. As shown the Δ values decrease up to 30 percent units, when measuring ^{154}Eu radiation instead of ^{137}Cs . The standard deviation increases more rapidly the larger number of rods being removed than in sections 5.1.1 and 5.1.2. The value of Δ decreases the more rods that are removed. Fig 17 also shows that s is smaller when the ^{154}Eu energy is used. For the chess-like pattern with 17 rods removed the standard deviation, s , is significantly larger than in the other cases. Still it should be easy to reveal this type of manipulation since the value of Δ_{max} is substantially lower than the mean activity. For measurements using ^{137}Cs a value $\Delta=0.5$ corresponds to more than five standard deviations.

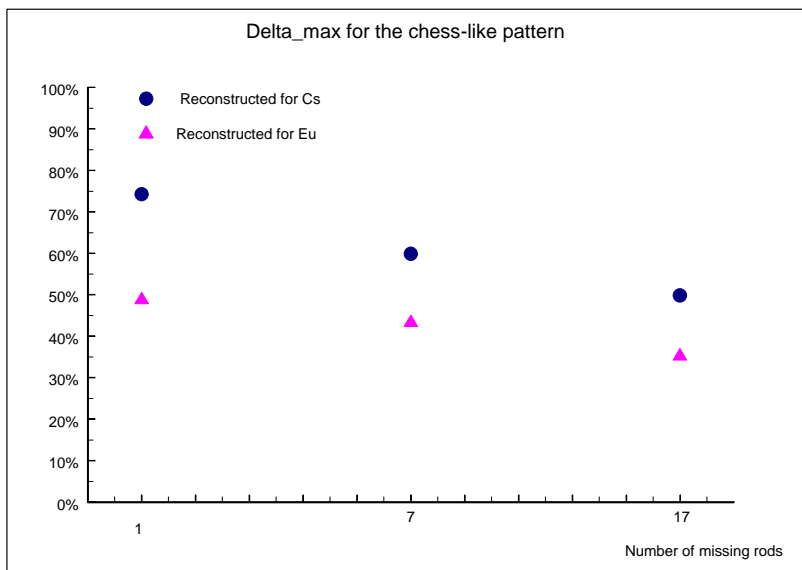
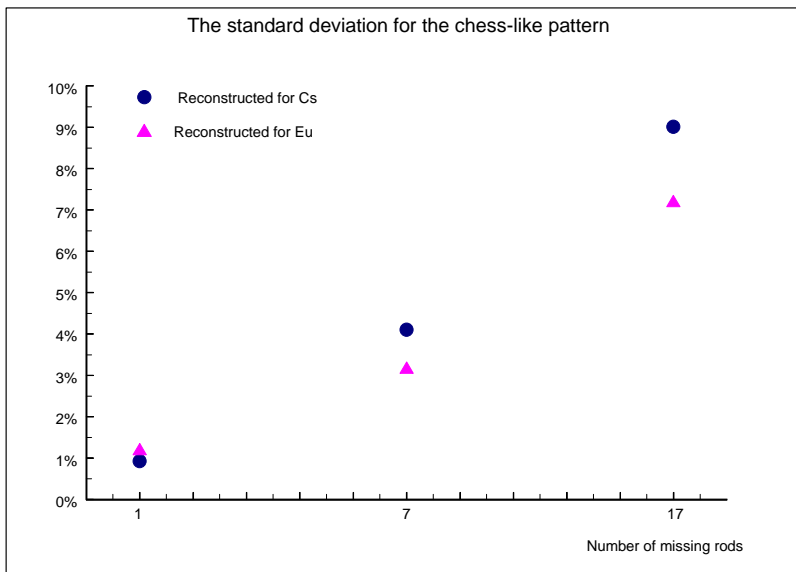


Figure 17 a) and b). The standard deviation and Δ_{max} for the three different configurations for both gamma energies. All simulations have been made for removed rods, 1200 detector positions and $N_{max} = 10000$ counts.

For neither of the three cases there was no difficulty to detect rods being replaced with fresh fuel. The standard deviation was below 1% in all three cases and no single Δ value was larger than 1.5%. This is in line with the expectation in section 2.3 that the reconstructed activity should be close to or equal to zero.

The reconstructed activities for case B are presented in fig. 18.

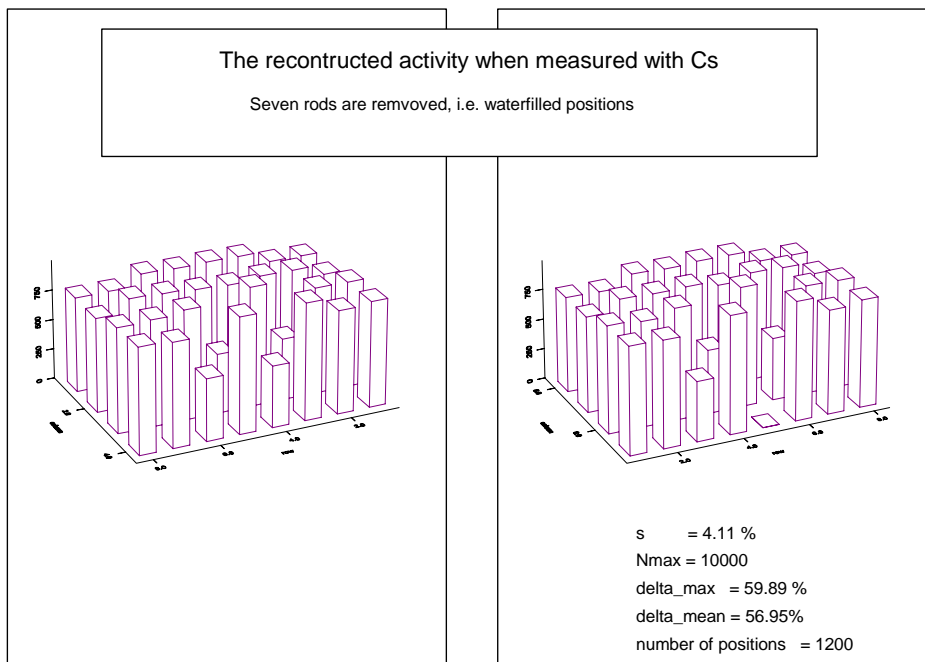


Figure 18. The reconstructed activity in each position when seven rods have been removed. The larger standard deviation is evident, since the activity values vary in the unaffected rods.

In fig. 18 the standard deviation was 4%, i.e. larger than in earlier presented cases. The value of Δ was below 60% which is in accordance with earlier simulations.

5.1.4 Comparison between the ^{154}Eu and ^{137}Cs gamma energies.

This study only concerns the case of removed rods. When replacing rods with fresh fuel both gamma energies yield Δ values close to zero. As shown in table 5 better results are obtained for simulations made with the ^{154}Eu gamma energy. This is especially true for rods removed in the inner positions.

In order to compare the ^{154}Eu and ^{137}Cs gamma energies, nine formations of removed rods have been investigated using simulated intensities with the same set of detector positions and statistics for both energies. Five concern one rod removed, three the chess-like patterns and one the inner section. Only investigations concerning water-filled positions have been made. The results are shown in the table below.

case considered	^{137}Cs	^{137}Cs	^{154}Eu	^{154}Eu	$^{154}\text{Eu}/^{137}\text{Cs}$	$^{154}\text{Eu}/^{137}\text{Cs}$
	Δ_{mean} [%]	Δ_{max} [%]	Δ_{mean} [%]	Δ_{max} [%]	s mean [%]	max [%]
The inner section	48.36	57.74	33.50	37.33	69.3	64.5
The chess-like pattern	74.28	74.28	49.01	49.01	66.0	66.0
	56.95	59.89	41.14	43.53	72.2	72.7
	44.52	49.84	30.30	35.42	73.0	71.1
One rod replaced	49.04	49.04	43.15	43.15	88.0	88.0
	51.42	51.42	43.56	43.56	84.7	84.7
	56.63	56.63	43.67	43.67	77.1	77.1
	64.80	64.80	47.48	47.48	73.8	73.8
	67.10	67.10	48.67	48.67	72.5	72.5

Table 5. Comparison between measurements with the ^{154}Eu and ^{137}Cs gamma energies. The two first cases in one rod missing concerns outer positions, while the three others concern inner positions just as the single rod in the chess-like pattern.

The table clearly shows that the tomographic image is improved using the higher gamma energy of ^{154}Eu . The effect is especially visible for the rods being removed from the central part of the assembly.

5.2 Rods removed or replaced in PWR fuel

The PWR fuel investigated here consists of 264 fuel rods and 25 water channels placed in a 17x17 matrix. The large number of rods makes reconstructions of PWR fuel more difficult than BWR since the gamma-ray penetration is lower, see table 2b). This is especially true for inner rods, because the radiation has to pass up to eight rods before escaping the assembly. This makes detection of removed or replaced rods in the inner parts of a PWR assembly more difficult. Table 2b) shows that for ^{137}Cs , about 1% of the intensity from an inner rod escapes the assembly. The corresponding fraction for ^{154}Eu radiation is about 8 %. This shows the considerable difference between the two energies, which could be a determining factor for the detection of removed or replaced rods. It is therefore of interest to use as high a gamma energy as possible.

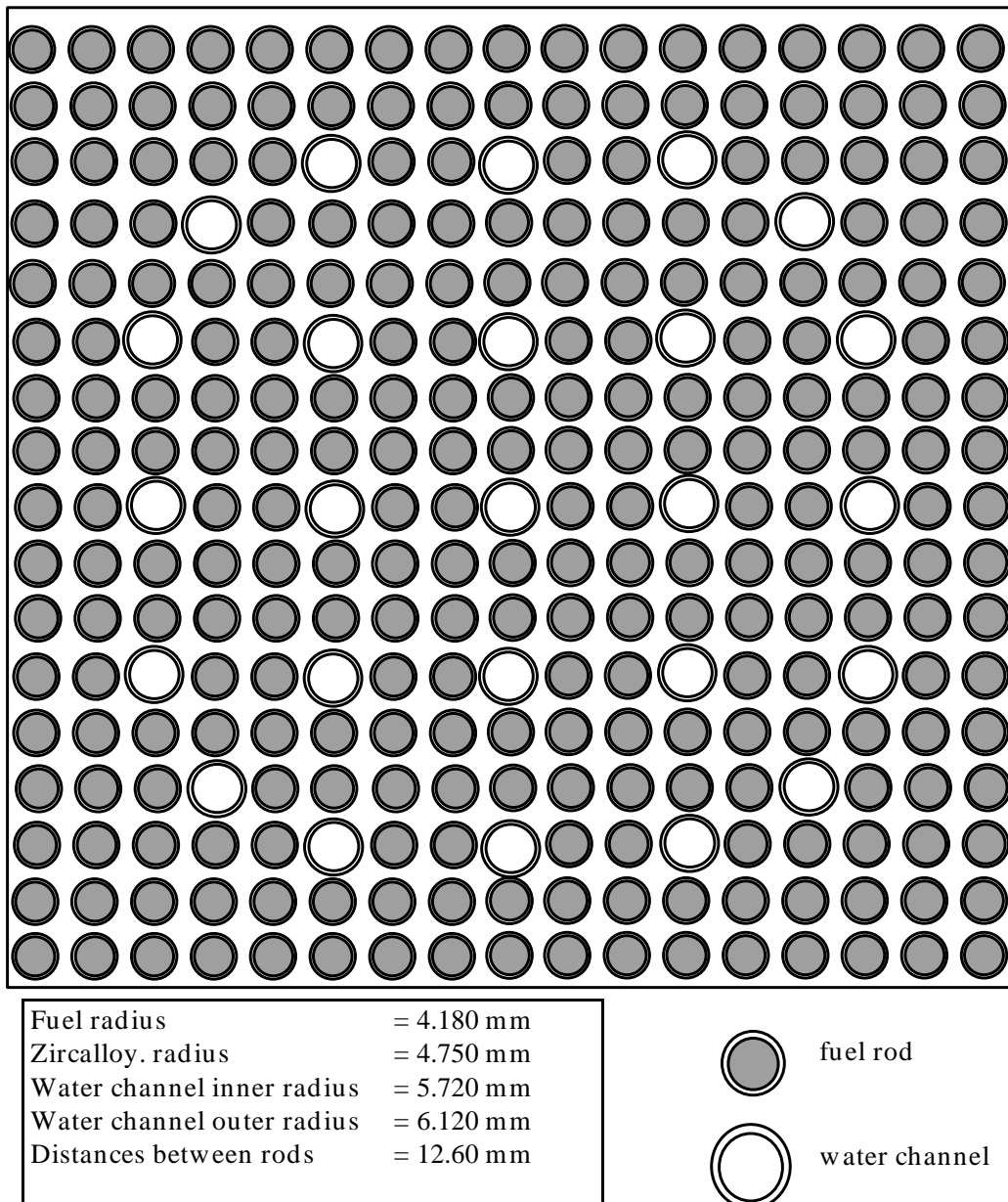


Figure 19. A schematic drawing of a 17x17 PWR fuel assembly. Each fuel rod has been assigned an individual number, the numbering start at the upper left corner. The simulated measurement equipment is described in section 3.1 .

Two cases of removed or replaced rods in PWR fuel have been examined. The first has treated single rods. The second formation correspond to groups of rods. In both formations it has been evident that the inner section is the most difficult to reconstruct accurately. Therefore the report is concentrated on those positions.

5.2.1 Single rods

Two configurations of removed or replaced rods have been examined which are shown in fig. 20.

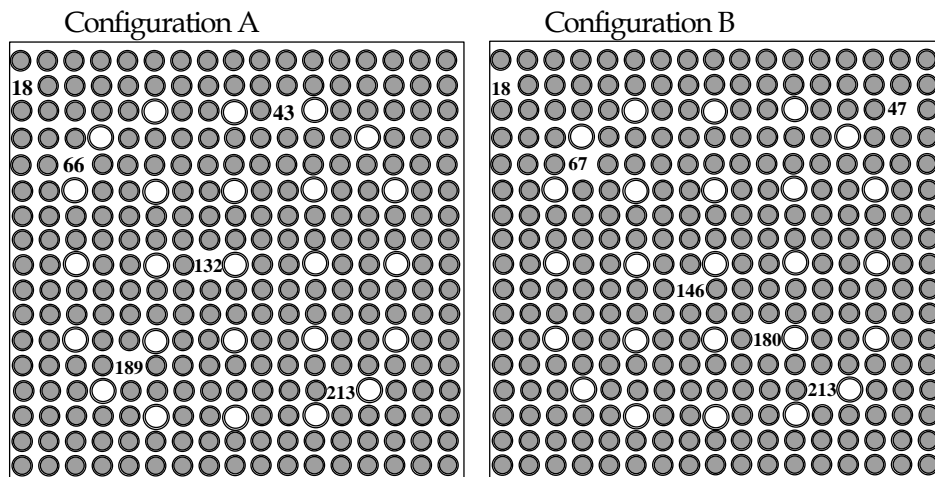


Figure 20. The two configurations for removal or replacement of single rods in PWR fuel. The numbers of the manipulated rods are indicated in the picture. The numbers only denote the fuel rods not the water channels.

The removal of rods.

Table 6 show some values of the reconstructed activities for rods being removed according to configuration A, when the average value is set to 1. Both tables show the region around the removed rod in position 132. The first case shows the results with ^{137}Cs and the second with ^{154}Eu . The results show that Δ of rod 132, the inner most position, was 89%. The corresponding value using ^{154}Eu was 64%. The standard deviation for ^{154}Eu was 1.5%, almost 1% unit smaller than for ^{137}Cs .

Configuration A

Some reconstructed activities, positions given, when using ^{137}Cs gamma energy .

1.04368	116	0.94108	117	1.00887	118
0.90486	131	0.90426	132	water channel	
1.03619	145	1.01089	146	1.03517	147

removed rod

Table 6 a) Some reconstructed activities using ^{137}Cs gamma energy. 1 corresponds to the mean value of all activities, i.e. including the activity of the replaced rods. The number of simulated positions are 3456 and $N_{max} = 100000$ counts.

Some reconstructed activities, positions given, when using the ^{154}Eu gamma energy.

1.02981	116	0.98879	117	1.00887	118
0.98838	131	0.64652	132	water channel	
1.01197	145	1.03152	146	1.03517	147

removed rod

Table 6 b) Some reconstructed activities using the ^{154}Eu gamma energy, to be compared to table 6a.

In the case of ^{137}Cs it is impossible to determine which rod that is removed since both the removed rod: 132 and its neighbour 131 has approximately the same relatively high reconstructed activity. In the case of ^{154}Eu , on the other hand, it becomes quite clear that rod number 132 has been removed and all others are intact.

Configuration B is similar to A, but the removed rods has slightly different positions. Some of the reconstruction values accounting for the region around the most central removed rod are presented in table 7.

Configuration B

Some reconstructed activities, positions given, when using ^{137}Cs gamma energy.

1.01115	131	0.97653	132	water channel
0.95286	145	0.88118	146	0.99813
1.00954	162	0.96435	163	0.98635

removed rod

Table 7 a) Some reconstructed activities using the ^{137}Cs gamma energy. Rods have been removed according to configuration B.

Some reconstructed activities, positions given, when using ^{154}Eu gamma energy.

0.97703	131	1.01479	132	water channel
1.02886	145	0.67357	146	1.04580
1.01507	162	0.98336	163	0.99074

removed rod

Table 7 b) Some reconstructed activities using the ^{154}Eu gamma energy. Rods have been removed according to configuration B.

It is obvious that Δ for the replaced rod is high for ^{137}Cs , but it may be possible to decide the position of the missing rod. When using the ^{154}Eu gamma energy the detection of the removed rod can be made more confidently.

The replacement of rods with fresh fuel.

The same configurations have been investigated for the case of replacing the rods with fresh fuel. For the innermost rods the obtained values of Δ was then up to about 10%. This value is larger than for BWR fuel, but still implies confident detection.

Comparison with BWR fuel

In the case of PWR the difference between Δ for ^{154}Eu and ^{137}Cs is up to 20 percent units, which is in accordance with the case of BWR. The standard deviation is approximately 1 percent unit lower in the ^{154}Eu case compared with the ^{137}Cs case. In both cases both Δ and s are considerably higher than in the case concerning BWR. For outer rods the values of Δ are more similar to the ones obtained for BWR. In PWR fuel the effect of the low penetrability of ^{137}Cs gamma rays is evident even in case of rods replaced with fresh fuel. The value of Δ for rods replaced with fresh fuel in the centre of the assembly increases to 10 %.

Investigations of the level of statistical noise.

The effect on s and Δ_{\max} when varying the value of N_{\max} are shown in Figure 21a and b. The results account for configuration B.

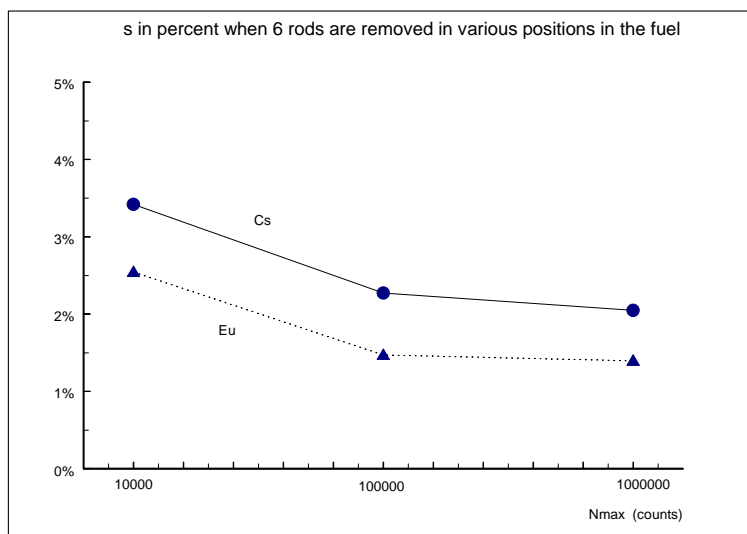
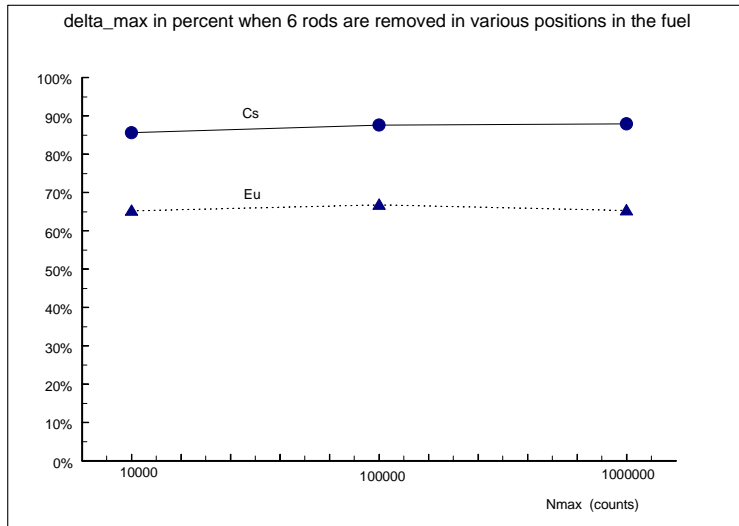


Figure 21 a) and b). The values of Δ_{\max} and s for configuration B for various values of N_{\max} .

In fig. 21a) the maximum value of Δ is displayed. It shows that the value using ^{137}Cs is substantially higher than the corresponding value for ^{154}Eu . The displayed Δ values are the highest reconstructed, thus they originate from the inner most rods. In b) the standard deviation in the corresponding cases are given. These show that s decreases as the number of N_{\max} increases. Figure 21 also shows that s is higher in PWR compared to BWR.

5.2.2 Groups of rods

A formation with two groups of removed or replaced rods have been simulated. The simulations have been made using both gamma energies. The configuration can be found in figure 22. The group in the inner section of the assembly consists of four rods, and the outer group consists of twelve rods.

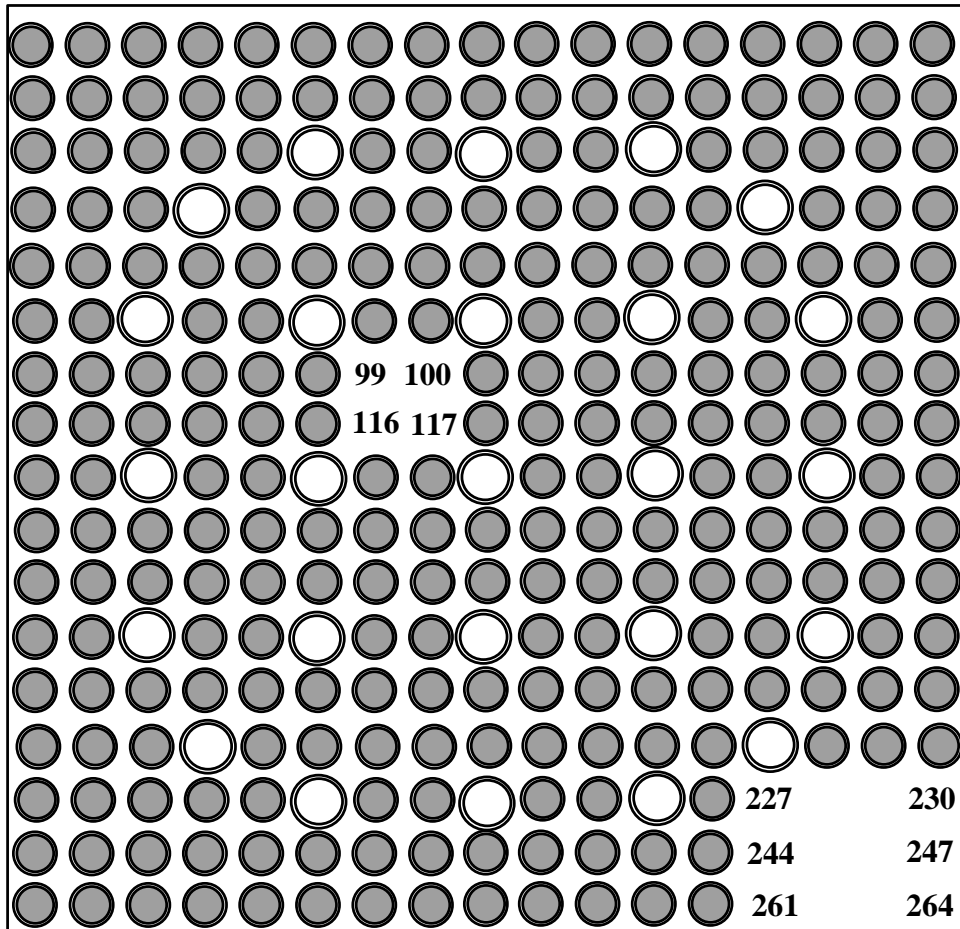


Figure 22. Schematic sketch of the simulated configuration with two groups of removed or replaced rods in a PWR assembly.

The results of the reconstructions can be found in figures 23 and 24. Some general features can be seen when examining the reconstructions. One is that Δ is lower in the outer regions, i.e. the values of Δ_{\max} accounted for in fig 23a and 24a correspond to the positions of the inner section. Another feature is that both the standard deviation and Δ are lower when using the ^{154}Eu energy.

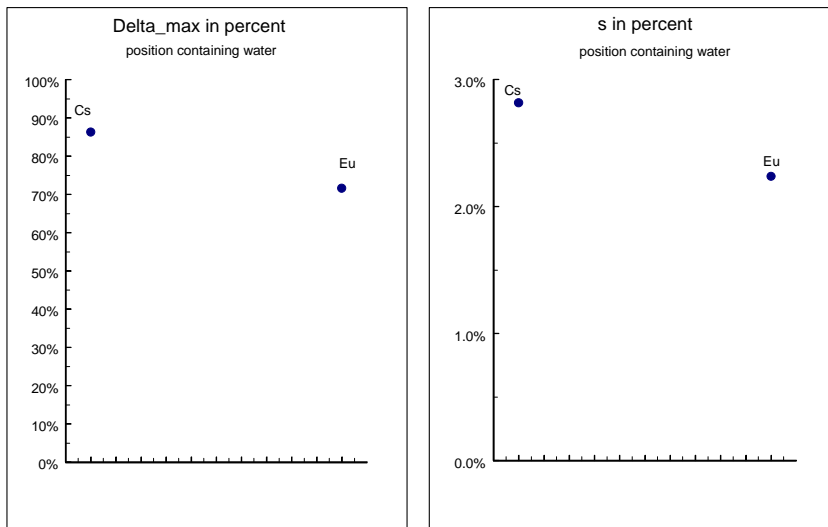


Figure 23 a) and b). Δ and s when the groups of rods are removed, i.e. correspond to water-filled positions. Both s and Δ are lower for the higher gamma energy of ¹⁵⁴Eu than for ¹³⁷Cs.

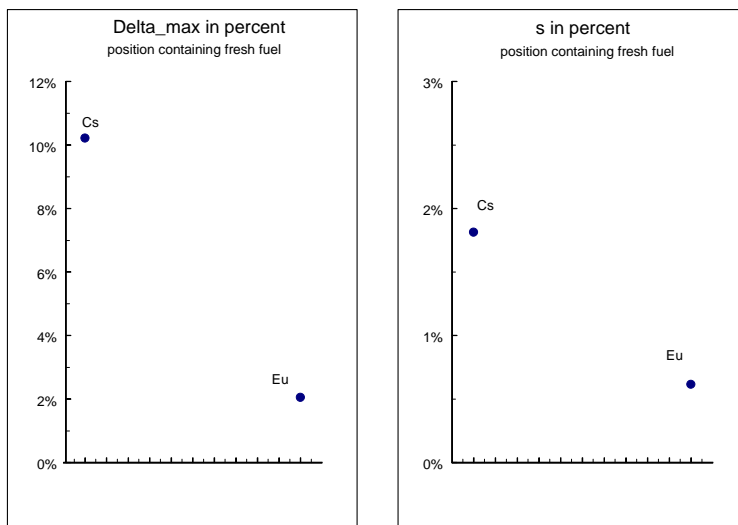


Figure 24 a) and b). Δ and s when the groups of rods correspond to rods replaced with fresh fuel. Also here s and Δ are lower for ¹⁵⁴Eu.

As shown in fig. 24 s is substantially lower for rods replaced with fresh fuel for both gamma energies compared to s for the positions containing water. The Δ values are for ¹³⁷Cs below 10.5 % and for ¹⁵⁴Eu below 2.5 %. This is in accordance with earlier results.

In figure 25a and b the Δ value of each rod is displayed for the case of removing the rods, i.e. water filled positions.

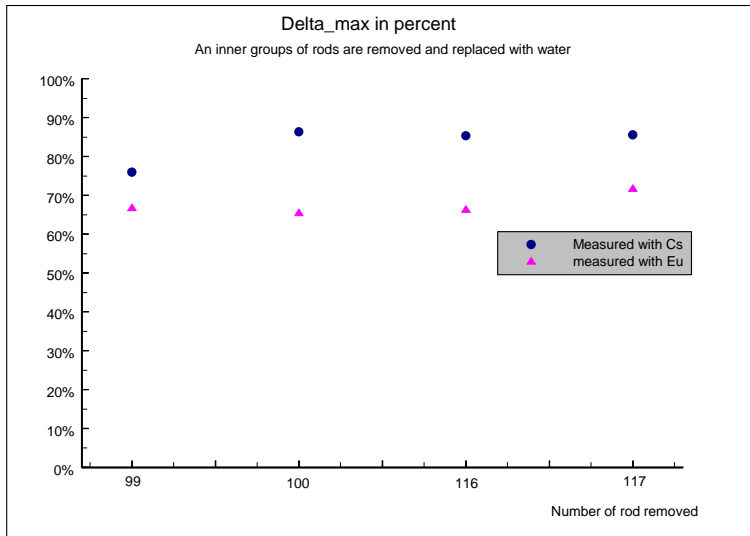


Figure 25. The Δ values of each removed rod in the inner group. The Δ values when measuring with Cs is 10-20 percent units higher than when measuring with Eu.

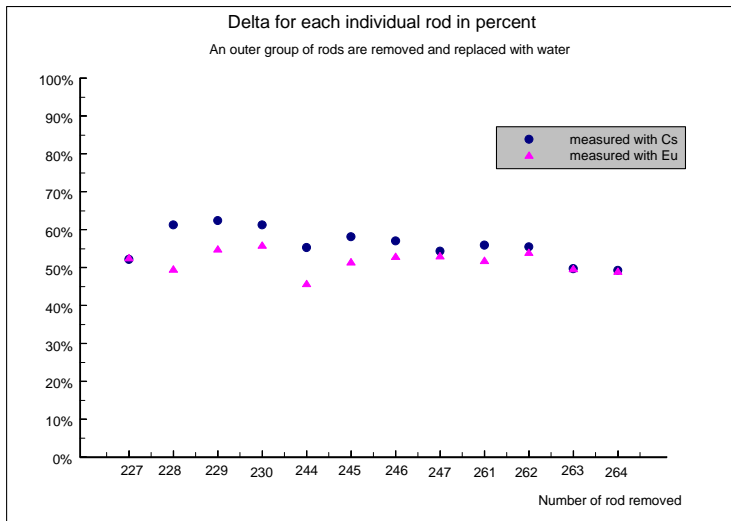


Figure 26. The Δ values of each removed rod in the outer group. Here the difference is small between measuring with ^{137}Cs or ^{154}Eu . These Δ values are smaller than the ones in fig. 25 corresponding to the inner rods. This can be explained by the smaller difference in the attenuation between ^{137}Cs and ^{154}Eu for the outer rods as discussed in chapter 2.3.

The outer group of removed rods has Δ values around 60 % for ^{137}Cs and 50 % for ^{154}Eu . The penetrability of the gamma rays is smaller from the inner section for which Δ is around 80 % for ^{137}Cs and 65 % for ^{154}Eu . Considering the results from especially the inner section it is desirable to use ^{154}Eu because it implies lower values of both s and Δ .

5.3 Comparisons between PWR and BWR

It is evident that it is a harder task to decide whether a rod is replaced or not in the PWR case compared to the BWR case. In both cases a rod replaced with fresh fuel should be easily detectable, since the reconstructed activity, Δ , has not been much higher than ten percent in any single case. This is in line with the assumption in section 2.3 that Δ for rods replaced with fresh fuel should be close to zero. In the case of removed rods it has not always been clear in every single case which rod has been removed. If the opportunity exists measurements at the higher gamma energy from ^{154}Eu will solve this problem.

The most difficult case to reveal for both PWR and BWR is when one single rod is removed. The reason for this is probably the small difference in the measured intensities such a removal gives rise to.

The removal of several rods in bundles decreases the individual Δ values, especially for BWR. In the PWR case this effect has not been as clear, but the Δ values were at least 4 standard deviations smaller than the mean, even when simulated using the ^{137}Cs gamma energy. In the case of BWR a chess-like pattern was also tested. The Δ values here was about 40-50%, but the standard deviation increased as the number of rods removed was increased. The reconstructed activity in any removed rod was anyway at least 4 standard deviations smaller than the mean activity.

Due to the large attenuation it is preferable to use ^{154}Eu . In both PWR and BWR Δ for positions of removed rods has been about 20-30 percent units lower for ^{154}Eu compared with ^{137}Cs . The difference has been most notable in the central parts of the assembly. In one of the simulated cases for PWR, it was impossible to decide which central position corresponded to a removed rod when using the ^{137}Cs gamma energy. Using the ^{154}Eu energy it became evident which position that was replaced.

The results in the case of PWR might be improved by using more measurement positions, but collecting more counts will not bring the standard deviation much lower. In fig 21b) the standard deviation decreases with about 0.2 % units when the number of N_{max} was increased from 100,000 to 1,000,000 counts.

Conclusions

The results of this study indicates the possibilities of detecting individual removed or replaced rods in nuclear fuel assemblies. To be able to draw reliable conclusions concerning removed rods in PWR fuel measuring gamma from ^{154}Eu is crucial because of the higher gamma-ray energy of this isotope. It was also shown in this work that the replacement of fuel rods with fresh fuel yields results of higher accuracy as compares to the case where the corresponding rods are replaced with water. This feature of the method is attractive from a Safeguard point of view.

References:

1. Ane Håkansson and Anders Bäcklin ;*Non-destructive assay of Spent BWR Fuel with High-Resolution Gamma-ray Spectroscopy*; Dept. of Radiation Sciences, Uppsala University 1995
2. Staffan Jacobsson; *Theoretical Investigations of Tomographic Methods used for Determination of the Integrity of Spent Nuclear Fuel*; TEKNIKUM Uppsala University 1996
3. Bertil Axelsson; *Quantitative SPECT, Studies of some Factors Influencing Quantitation Accuracy in Single Photon Emission Computed Tomography*; Dep. of Radiation Physics, Stockholm University 1987
4. A.C Kak, M. Slaney; *Principles of Computerised Tomographic Imaging*; IEEE Press, New York 1988
5. C. Norling, J. Österman; ”*Physics handbook*”; Studentlitteratur, Lund 1982
6. NEA Data Bank; Program ZZ-XCOM; 1991; Page-ID: DLC-0174/01 (<http://www.cea.fr/abs/html/dlc-0174.html>)
7. B. Grapengiesser et. al.; ”*Kompendium i Kärnbränsleteknik*”; ASEA-Atom (ABB) 1985

Acknowledgments:

This work has been financed by the Swedish nuclear power inspectorate, SKI. The author also wishes to thank the two supervisors Ane Håkansson and Staffan Jacobsson, and Anders Bäcklin and Peter Jansson, for all their support, all four works at the Department of Radiation Sciences at Uppsala university.